JOURNAL OF RESEARCH of the National Bureau of Standards — A. Physics and Chemistry
Vol. 75A, No. 6, November-December 1971

An Absolute Determination of Viscosity Using Channel Flow

Robert W. Penn and Elliot A. Kearsley

Institute for Basic Standards, National Bureau of Standards, Washington, D.C. 20234

(July 28, 1971)

The viscosity of a sample of di(2-ethylhexyl) sebacate has been determined by measuring the pressure at taps along a closed channel containing the flowing liquid. By means of relative viscosity measurements in conventional capillary viscometers, we are able to express our results in terms of the viscosity of water at 20 °C. We find a value of 0.010008 poise. An appendix outlines the calculation of upper and lower bounds for the geometrical flow constant.

Key words: Absolute measurement; calculation of bounds; calibration; Poiseuille flow; standard; viscosity; viscous flow.

1. Introduction

The history of the absolute measurement of the viscosity of water at the National Bureau of Standards began about 1931 when a committee chaired by E. C. Bingham recommended that a new determination be made. Work proceeded spasmodically until 1952 when Swindells, Coe, and Godfrey [1][1] published the results of their work, and the recommended value for the viscosity of water at 20 °C was changed from 1.005 centipoise (cP) to 1.002 cP. In 1957 Kearsley pointed out that all of the previous measurements had been made by very similar experiments and that there was a possibility that an unknown systematic error affected all of the results. At that time work was started on two different absolute measurements. One of these involved measuring the period of a liquid-filled sphere oscillating in torsion. The other involved measuring the pressure at taps along a capillary. Work proceeded, again spasmodically, on both of these experiments. In 1959, Kearsley published the analysis of the torsional sphere viscometer [2]. Results of that work are presented in an adjacent paper [3]. In 1968 we decided to construct an accurate channel in order to avoid some of the difficulties of measuring the radius and radius distribution of small capillaries. At the suggestion of Mr. T. R. Young of the Metrology Division we settled on a channel formed by pressing two cylindrical rods against a flat plate. This suggestion led to the work which we report here.

2. Experimental Procedure

Figure 1 shows a cross section of the channel we used. Two 2-cm diameter stainless steel rods were clamped against a 2-cm thick plate glass flat and sealed with epoxy resin to produce a cuspoid-triangular channel one meter long. This geometry allowed us to put the pressure taps out in the corners of the channel in a region of low velocity so that any disturbance of the flow would be minimized. The new geometry required us to calculate the geometrical flow constant. This was accomplished by computer calculation of upper and lower bounds, which agreed to better than five significant figures. Details of this calculation are presented in appendix 1.

The channel was placed in the apparatus shown in figure 2. A large, well insulated, water filled thermostat was constructed. The channel was fed from a water jacketed stand pipe which produced a constant pressure head. The stand pipe was fed by a pump which took the oil (a commercial grade of di(2-ethylhexyl) sebacate) from a large reservoir through an oil filter, then through a 50 ft coil of copper tubing to bring the oil to the bath temperature, and then to the top of the stand pipe. Overflow returned to the reservoir.

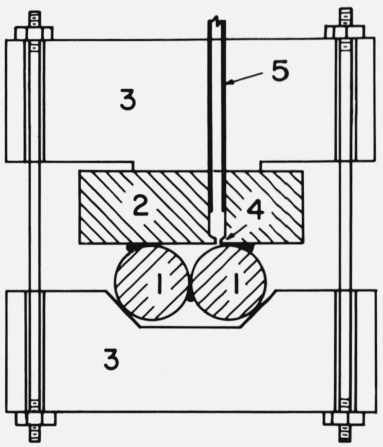

FIGURE 1. *Cross section of channel assembly.*

1, Stainless steel rods. 2, Plate glass flat. 3, Plastic clamps. 4, Pressure tap. 5, Copper tubing to pressure gage.

[1] Figures in brackets indicate the literature references at the end of this paper.

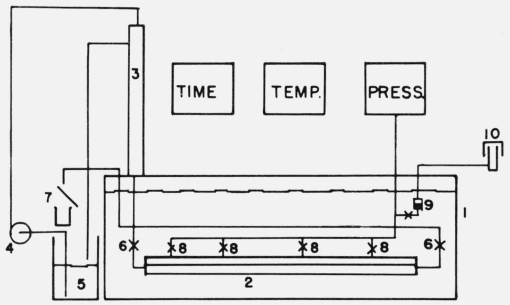

FIGURE 2. *Schematic diagram of the channel flow assembly.*

1. Thermostat. 2, Channel assembly. 3, Water jacketed stand pipe. 4, Pump. 5, Oil reservoir. 6, Flow control valves. 7, Solenoid operated diverter. 8, Pressure tap valves. 9, Oil-air interface. 10, Dead weight piston gage.

The channel was fed from the standpipe by plumbing which allowed us to run the flow in either direction. The flow was controlled by a needle valve near the entrance end of the channel. The effluent was returned to the reservoir. A solenoid operated device was used to divert the effluent stream so that accurately timed samples could be taken in beakers for weighing.

The measurement of pressure transmitted through the small pressure taps (0.08-cm diam) required the use of a high impedance pressure gage. A liquid filled fused quartz bourdon tube was used. This gage could be connected to any one of the four pressure taps to measure its pressure with respect to the efflux tube level by opening the tap valves one at a time. By closing all of the tap valves and opening the connection to an oil air interface, the quartz bourdon gage could be connected to a dead weight piston gage for calibration before and after a series of test runs.

Temperature was controlled by a proportional controller which balanced an electric heater against the heat loss to a constant temperature cooling coil. Temperature was measured with a quartz crystal thermometer which was calibrated against a platinum resistance thermometer before and after a series of test runs.

We now have all of the quantities necessary to calculate the kinematic viscosity of our test fluid:

$$\nu=\frac{\Gamma\Delta PR^4T}{LM}. \tag{1}$$

Γ is the (dimensionless) geometrical constant, 3.64872×10^{-3}; $\Delta P/L$ is the pressure gradient; R is the radius of the rods; M is the mass of fluid flowing in time, T; and ν is the kinematic viscosity, the viscosity divided by the density.

3. Discussion of Errors

Figure 3 shows the final results for measurements taken on two days in two directions of flow with four different flow rates from 1.5 to 5.2 g/s. These rates correspond to Reynolds numbers between 6.5 and 22. A detailed display of data is included in appendix 2. A statistical analysis of the pressure measurements show: (1) There is no significant day-to-day variation; (2) The variability of the individual pressure measurements does not correlate with flow rate; (3) There is no difference in average gradient for the two directions; (4) There is a statistically significant correlation of viscosity with flow rate for the left to right direction but not for the right to left direction. The total spread of the data in figure 3 is 0.06 percent of the mean. The standard deviation of their average is only 0.02 percent. In order to estimate the absolute accuracy of the measurements, we will examine the accuracy with which we know each of the various factors in eq 1.

3.1. The Geometrical Flow Constant

As mentioned above, we have calculated the geometrical factor to five significant figures. We have three ways to estimate how well we realized the geometry. The first was obtained from measurements of the diameters of the rods along four different diameters at thirteen places on the rods. The measurements were made by comparison with a gage block which was calibrated by the Length Measurements Section. Its dimension was known to within $\pm10^{-6}$ inches. The comparison was made using a dial gage with a precision of $\pm10^{-5}$ inches. The two rods differ in average diameter by 10^{-4} in. This difference would produce only a negligible error in the area of the channel and in the calculated viscosity. The diameter measurements show a standard deviation of 6×10^{-5} in and a maximum range of 3×10^{-4} in. The reciprocal of the root mean fourth power of the reciprocal diameters is found to be the same as the mean diameter to seven significant figures. From the standard deviation in diameter we calculate an uncertainty in viscosity of 0.032 percent due to the uncertainty in the value of R. This does not include the effects of radial flows due to irregularities in the cross section which we do not know how to estimate.

A second estimate of the accuracy of the geometry of the channel was obtained from an examination of the optical interference pattern between the rods and plate with sodium light which showed the distance of separation due to irregularities. Figure 4 shows a typical interference pattern. The rods were clamped to the glass plate by means of 12 equally spaced plastic [2]

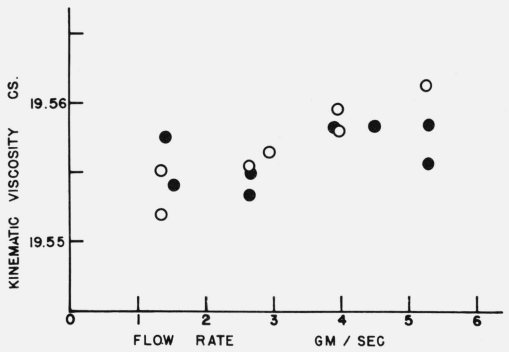

FIGURE 3. *Kinematic viscosity of oil sample at various flow rates.*
Closed circles, flow right to left. Open circles, flow left to right.

[2] Plastic components of the apparatus were constructed from commercially available poly(methyl methacrylate) materials.

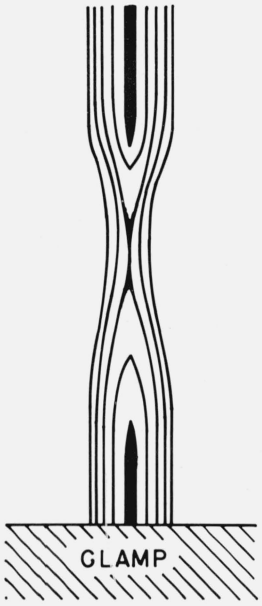

FIGURE 4. *Typical interference pattern between a steel rod and the glass plate showing second order separation.*

clamps 2-cm wide. Invariably, the zero order fringe indicated intimate contact between rods and plate in the regions under the clamps and within 1 cm of a clamp. Of the remaining 52 cm of the channel, the first, second, third, and fourth order fringes closed in about 26 cm, 14 cm, 10 cm, and 2 cm, respectively. By taking a weighted average of the reciprocals of the squares of the cross sections augmented by such separation, one estimates that the observed viscosity would be reduced by 0.025 percent. It is not clear how these separations are related to the variations in diameter of the rods, to nonstraightness of the rods, or to nonflatness of the glass plate.

Finally, using linear elasticity theory, we can estimate the penetration of the rods into each other and into the glass plate. These effects could reduce the cross-sectional area of the channel by less than 10^{-4} percent and so produce an error of less than $\pm 2\times 10^{-4}$ percent in viscosity. Such penetration would, of course, tend to compensate for errors due to separation which were observed by means of the optical interference patterns. One cannot say with certainty how much these irregularities will disturb the flow; however, we estimate that we know the geometry of the channel well enough to assign an uncertainty of ± 0.04 percent from these sources.

3.2. Flow Rate Measurements

Uncertainties in flow rate can be estimated in several ways. First, duplicate determinations made before and after a series of pressure measurements show a standard deviation of 0.01 percent. Second, uncertainties in weighing 100- to 500-gram samples using calibrated weights are less than ± 0.005 percent. Our time interval measurements were made with a digital counter controlled by the National Bureau of Standards' standard frequency. Therefore the uncertainty in the time required to move the diverting mechanism constitutes the principal timing error.[3] From measurement of the mass of this mechanism and the forces used to move it we calculate that it takes about 0.02 s to move the diverter between its on and off positions. The flow during 0.02 s is 0.02 percent of the total flow. The uncertainty in flow rate due to the timing error is certainly less than this.

3.3. Pressure Gradient Measurements

Errors in the pressure gradient measurement could arise from errors in measurements of pressure, from uncertainty in measurements of the distances between the pressure taps, or from irregularities in the cross section of the channel, such as a possible constriction between two of the taps.

a. Distances Between Pressure Taps

The distances between the pressure taps in the glass plate were measured with a cathetometer. The cathetometer was checked against a standard Invar meter in 1952 with no correction larger than 10^{-3} cm. The midpoints of the holes were located to within $\pm 2\times 10^{-3}$ cm from an arbitrary reference point near one end of the channel. The holes were approximately 0.08 cm in diameter. Since we wish to determine a pressure gradient, we have assumed that we measure the pressure at each of the holes at the same point with respect to its midpoint. We then determine the pressure gradient by a least squares technique of fitting the pressure measurements to a linear function of distance along the channel. The same values of pressure gradient are obtained to six digits whether the errors are attributed to pressure measurements or to measurements of position of the holes. The statistical analysis of the pressure measurements indicates that there is a barely significant systematic deviation of the individual pressure measurements from the constant gradient line. The pressure reading deviations from the center two taps are consistently positive for one direction of flow and negative for the other direction. These deviations from the constant gradient line could be explained by uncertainties of 8×10^{-3} cm in the position of the holes. This is approximately one-tenth of the diameter of the holes. Deviations from this source are indistinguishable from those due to irregularities in the cross section of the channel.

b. Pressure Measurements

Pressure measurements were made with a liquid filled, fused quartz bourdon gage with a resolution of about ± 0.1 N/m^2. Pressure measurements were reproducible to within ± 0.1 N/m^2 both during the viscosity measurements and during the calibration of this gage against a dead weight piston gage. The effective area

[3] The diverter was removed from the oil stream during the timed period, thus drainage from it did not contribute to error.

of the piston gage certified by the manufacturer, and checked by the Pressure Measurement Section of NBS, is within 0.01 percent of its nominal value. The weights used were found to be accurate within 0.005 percent of their nominal values.

Since air was used in the piston gage, the calibration was made through an oil-air interface of 4-cm diameter which might introduce an uncertainty of ± 0.1 N/m^2 due to surface tension effects. A reproducible periodicity of ± 0.5 N/m^2 amplitude in the calibration curve was traced to the gears in the system used to measure the angular displacement of the quartz bourdon tube. The calibration curve was found to be reproducible over the period of the measurements to within ± 0.15 N/m^2, or ± 0.03 percent for the smallest pressure differences measured.

Since all of the systematic deviations of pressure measurements from the constant gradient line are barely significant statistically, we have chosen to use an average of all of the pressure gradient determinations weighted by the inverse of their individual standard deviations. The standard deviation of this average is only 0.02 percent. We estimate the absolute accuracy of this average to be ± 0.06 percent.

3.4. Temperature Measurements

Temperature was controlled in the thermostat at 25 °C by means of a proportional controller with reset action which uses a platinum resistor as a sensing element. Temperature was measured with a digital thermometer which uses a quartz crystal as a sensing element. This thermometer indicated temperature within the bath constant to $\pm 10^{-3}$ °C for periods up to 8 hr. Rapid temperature fluctuations of about ± 0.003 °C were found at the end of the bath near the heater and cooling coil. The average temperature here was the same as that of the rest of the bath. The digital thermometer was calibrated against a platinum resistance thermometer in a well stirred oil bath. The platinum thermometer had been calibrated in 1960 in terms of the International Temperature Scale of 1948. A triple point temperature check and bridge calibration were made in 1969.

Temperature measurements were made both in the circulating bath and in copper temperature wells, shown in figure 5, which had good thermal contact with the test oil but were relatively isolated from the water of the bath. These wells were placed in the oil stream at both ends of the channel. No significant difference was found between the two wells; however, both well temperatures consistently read 0.004 °C higher than the bath temperature. The same difference was found whether or not oil was flowing in the channel. It was attributed to self-heating of the temperature probe in the unagitated water in the wells. We believe we know the temperature of the oil to better than ± 003 °C which would produce an uncertainty in viscosity of ± 0.012 percent.

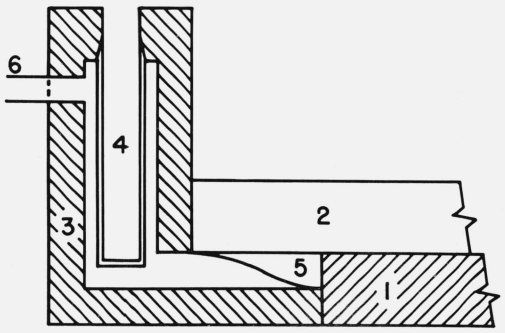

FIGURE 5. *Diagram of channel entrance section.*

1, Steel rod. 2, Plate glass flat. 3, Plastic entrance adapter. 4, Copper thermometer well. 5, Plastic streamline fillet. 6, Oil entrance tube.

3.5. Summary of Error Estimation

We list in table 1 the various sources of error which we have considered. These errors can be combined to a total probable error of approximately ± 0.1 percent.

TABLE 1. *Systematic errors*

Error source	Estimated accuracy
	Percent
Geometry of channel	± 0.04
Flow rate	± 0.02
Pressure measurements	± 0.06
Temperature measurements	± 0.012
Total absolute value	± 0.13
Root total squares	± 0.075

One effect which might be expected in these measurements is that the pressure at the hole nearest the entrance end of the channel might deviate from the others due to entrance effects. This effect is apparently seen in a significant dependence of pressure gradient on flow rate for left to right flow direction where the first hole is only 7 cm from the entrance. We attempted to minimize this effect by streamlining the entrance to the channel with plastic fillet pieces shown in figure 5. No effect is seen for right to left flow where the first hole is 28 cm from the entrance. Eliminating this effect by leaving out the data from the first hole would increase our final result by only 0.01 percent.

Corrections were applied to the raw data for air buoyancy on the weights of oil samples and on the weights used in calibrating the pressure gage. The local acceleration of gravity was calculated from the value determined by Tate [4] assuming a gravity gradient of 3×10^{-6}s^{-2}. Temperature corrections were applied using a decrement of 4 percent per degree which was determined in a capillary viscometer.

4. Results

The direct result of this work is a value for the kinematic viscosity of one sample of commercial grade di(2-ethylhexyl) sebacate at 25 °C. This value was found to be 19.555 centistokes. By means of conventional relative viscosity measurements [5], this value can be compared with the viscosity of water at 20 °C. Such measurements were made immediately before and after our absolute measurements. Neglecting errors in the relative viscometry, we calculate the

viscosity of water of 20 °C to be 1.0008±0.0010 centipoise (cP). The corresponding value from the torsional sphere viscometer [3] is 1.006±0.001 cP. The discrepancy suggests the presence of an unidentified systematic error in one or both of these measurements of at least 0.25 percent. The comparison is discussed in detail by Marvin [6].

We gratefully acknowledge the assistance of many members of the staff of NBS. Particularly, we would like to thank Marion Brockman, who assisted with many of the measurements, Henry Pierce, who made density and relative viscosity measurements, and James Filliben of the Statistical Engineering Section, who assisted with the analysis of our results.

5. Appendix 1. Calculation of Bounds for the Geometrical Flow Constant

For unaccelerated viscous flow of an incompressible fluid through a channel the Navier-Stokes equations may be reduced to:

$$\nabla^2 v=\frac{1}{\eta}\frac{dP}{dz}=-K \qquad \text{(A–1)}$$

where $v(x, y)$ is the velocity profile, η is the viscosity, dP/dz is the pressure gradient in the direction of flow, and K is a positive constant. The total flow

$$Q=\int_S v dS \qquad \text{(A–2)}$$

over the cross-sectional area, S, of the channel. By Green's Theorem, since $v=0$ on the boundary, by the adherence condition

$$\int_S (v\nabla^2 v+\nabla v\cdot\nabla v)dS=\int_\beta v\nabla v\cdot d\beta=0 \qquad \text{(A–3)}$$

where β is the boundary of the channel, and $d\beta$ is in the direction of the outward normal. Combining equations (A–1), (A–2), and (A–3), we obtain

$$Q=\frac{1}{K}\int_S \nabla v\cdot\nabla v dS. \qquad \text{(A–4)}$$

From equations (1) and (A–1) which define Γ and K, respectively,[4] it is possible to express the relationship between K and Γ as

$$\Gamma=\frac{Q}{KR^4}. \qquad \text{(A–5)}$$

[4] The equations $M/T\rho=Q$ and $\Delta P/L=-\partial P/\partial z$ relate the quantities of the two equations.

Since Γ is a dimensionless geometric constant, we can arbitrarily set K and R equal to one and Γ will be numerically equal to the corresponding value of Q.

5.1. Upper Bound

To obtain an upper bound for Q, one chooses a trial velocity function, ψ, which satisfies the differential equation (A–1), but does not necessarily satisfy the boundary condition. Then, by Green's Theorem and the adherence condition

$$\int_S (v\nabla^2\psi+\nabla v\cdot\nabla\psi)dS=\int_\beta v\nabla\psi\cdot d\beta=0. \qquad \text{(A–5)}$$

By Schwarz' inequality:

$$K\int_S v dS=\left|\int_S (\nabla v\cdot\nabla\psi)dS\right|$$

$$\leq\left(\int_S(\nabla v\cdot\nabla v)dS\cdot\int_S(\nabla\psi\cdot\nabla\psi)dS\right)^{1/2}$$

$$KQ\leq\left(KQ\cdot\int_S(\nabla\psi\cdot\nabla\psi)dS\right)^{1/2}$$

$$Q\leq\frac{1}{K}\int_S(\nabla\psi\cdot\nabla\psi)dS. \qquad \text{(A–6)}$$

Equation (A–6) defines an upper bound for the total flow.

5.2. Lower Bound

To generate a lower bound for Q one chooses another trial velocity function, φ, which satisfies the boundary condition, $\varphi=0$ on β, but does not necessarily satisfy the differential equation (A–1). Then, by Green's Theorem:

$$\int_S(\varphi\nabla^2 v+\nabla\varphi\cdot\nabla v)dS=\int_\beta\varphi\nabla v\cdot d\beta=0 \qquad \text{(A–7)}$$

since $\varphi=0$ on β. Again, by Schwarz' inequality

$$\left(K\int_S\varphi dS\right)^2=\left(\int_S(\nabla\varphi\cdot\nabla v)dS\right)^2$$

$$\leq\int_S(\nabla\varphi\cdot\nabla\varphi)dS\cdot\int_S(\nabla v\cdot\nabla v)dS$$

$$\frac{\left(K\int_S\varphi dS\right)^2}{\int_S(\nabla\varphi\cdot\nabla\varphi)dS}\leq\int_S(\nabla v\cdot\nabla v)dS=KQ.$$

Thus,

$$\frac{K\left(\int_S \varphi dS\right)^2}{\int_S (\nabla\varphi \cdot \nabla\varphi) dS} \leq Q \qquad \text{(A-8)}$$

which defines a lower bound for the total flow.

5.3. Optimization of Bounds

For the upper bound we can choose as a trial function

$$\psi = by^2 + \Sigma\alpha_n h_n \qquad \text{(A-9)}$$

where $b = K/2$, α_n is an arbitrary coefficient and h_n is a harmonic polynomial of degree n in x and y.

$$\nabla^2 h_n = 0.$$

There are two such polynomials of each degree; one is even and one is odd in y. In the present problem we may choose our axes such that the channel is symmetric about the x axis, with origin at the point of contact between the cylinders. Then we need not include the polynomial which is odd in y.

The integral

$$Q_U = \frac{1}{K}\int_S (\nabla\psi \cdot \nabla\psi) dS$$

will be quadratic in the $\alpha_n's$. Q_U can be written in matrix component notation with the usual summation convention as:

$$KQ_U = \alpha_l H_{lm}\alpha_m + 4b\alpha_l Y_l + 4b^2 \int_S y^2 dS \qquad \text{(A-10)}$$

where the arbitrary coefficients α_n form a vector; H is the symmetric matrix,

$$H_{nm} = \int_S \left(\frac{\partial h_n}{\partial x}\frac{\partial h_m}{\partial x} + \frac{\partial h_n}{\partial y}\frac{\partial h_m}{\partial y}\right) dS;$$

and Y is a vector,

$$Y_n = \int_S \left(y\frac{\partial h_n}{\partial y}\right) dS.$$

To find the values of the arbitrary coefficients which minimize Q, we differentiate eq (A-10) with respect to α and set the derivatives equal to zero to obtain

$$K\frac{\partial Q_U}{\partial \alpha_i} = 2H_{il}\alpha_l + 4bY_i = 0. \qquad \text{(A-11)}$$

We can solve for the coefficient vector,

$$\alpha_i = -2bH^{-1}_{il}Y_l.$$

This result can be put into eq (A-10) to yield the desired upper bound.

For the lower bound, we can choose a trial function

$$\varphi = F \cdot G$$

where F is a function which vanishes on the boundary β and G is an arbitrary function. We have used[5]

$$F = (x^2+y^2-2y)\ (x^2+y^2+2y)\ (x-1)$$

and

$$G = \sum_{i,j=0}^{n,m} a_{ij}x^i y^{2j}.$$

Then, since F vanishes on β,

$$\frac{Q_L}{K} = \frac{\left(\int_S FG dS\right)^2}{\int_S (G^2\nabla F \cdot \nabla F - F^2 G\nabla^2 G) dS} \qquad \text{(A-12)}$$

is the functional to be maximized by adjusting the a_{ij}'s. This can be done by minimizing the denominator under the condition that

$$\int_S FG dS = 1$$

by Lagrange's method of undetermined multipliers. If we call the denominator of (A-12) D *and* $\int_S FG dS = N$ then

$$\frac{\partial D}{\partial a_{ij}} + \lambda\frac{\partial N}{\partial a_{ij}} = 0 \qquad \text{(A-13)}$$

$$N = 1$$

form a set of $(n+1)\ (m+1)+1$ equations which are linear in the a_{ij}'s. If we relabel a_{ij}:

$$a_{ij} = \alpha_{(m+1)i+j},$$
$$\lambda = \alpha_{(n+1)\,(m+1)}$$

then eqs (A-13) can be written as

$$\left|\begin{array}{c|c||c|c|c} \dfrac{\partial^2 D}{\partial\alpha_i\partial\alpha_j} & \dfrac{\partial N}{\partial\alpha_i} & & & 0 \\ & & & & 0 \\ & & & & 0 \\ & & \alpha_i & = & \cdot \\ \hline & & & & \cdot \\ & & & & \cdot \\ \left(\dfrac{\partial N}{\partial\alpha_i}\right)^T & 0 & & & 1 \end{array}\right| \qquad \text{(A-14)}$$

where the matrix on the left is indicated as a par-

[5] This F is the lowest order polynomial which vanishes on β. It is important that F does not vanish within S in order that the bound given in (A-12) be a close one.

titioned matrix. The problem is thus reduced to finding the inverse of this matrix and from that to calculate the optimum α_n's through (A–14) and then the bound through (A–12). In fact, the element at the bottom of the diagonal of this inverse matrix is the reciprocal of the bound.

For both of the bounds the matrix elements involved are composed of sums of integrals of the form

$$I_{nm} = \int\int x^n y^m dy dx$$

over the cross-sectional area of the channel. This integral can be expressed as a sum of beta functions [7] since:

$$I_{nm} = B_{nk} C_{km}$$

where

$$C_{km} = \frac{(-1)^k (m)!}{(m-k+1)!\,k!}$$

and

$$B_{nk} = \mathrm{B}\left(\frac{n+1}{2}, \frac{k}{2}+1\right) = \frac{\Gamma\left(\frac{n+1}{2}\right)\Gamma\left(\frac{k}{2}+1\right)}{\Gamma\left(\frac{n+k+3}{2}\right)}.$$

Both of these calculations were coded for the UNIVAC 1108 computer. With the inclusion of the first 21 harmonic polynomials for the upper bound and 31 terms up to x^5y^8 in the lower bound calculation, the two bounds converged to 3.64872 ($\pm$0.00002) $\times$ 10^{-3}

6. Appendix 2. Data

Tables A1 and A2 show flow rate and pressure data taken on two days. Table A3 lists measurements of the distances of the midpoints of the four pressure taps from one end of the channel. The individual masses of oil listed in tables A1 and A2 have not been corrected for air buoyancy. The average flow rates have been so corrected. The appropriate factor is 1.0012. The pressure measurements have been corrected for the nonlinearities in the quartz bourdon gage. They have not been corrected for the local gravity of 980.0972 cm/s^2 nor for air buoyancy on the calibrating weights. The appropriate factor is 0.99927. The viscosity values listed should also be so corrected. They are shown in the table for the operating temperature of 25.035 °C. They should be multiplied by 1.0014 to adjust them to 25 °C. The appropriate factor to convert the pressure gradient-flow rate ratios to kinematic viscosity is 207.404.

Run number eight gave a value of viscosity more than three standard deviations from the average of the other fifteen runs. Although we could find no reason for this difference we have assumed that it is not due to random error and we have not included it in our final average.

TABLE A1. *Flow rate and pressure data for day 1.*

Flow direction			Right to left				Left to right			
Run number			2	4	5	7	1	3	6	8
	Nominal		1.5	3	4.5	6	1.5	3	4.5	6
	Mass (g)		132.141	254.568	371.234	565.633	128.786	252.383	379.414	510.885
	Time (s)		95.36	96.89	95.48	107.42	95.13	95.24	96.09	97.68
Flow Rate, g/s	Mass (g)		147.660	285.531	411.833	534.506	142.801	315.619	416.731	530.851
	Time (s)		106.57	108.67	105.91	101.51	105.58	118.98	105.55	101.51
	Average		1.3873	2.6306	3.8929	5.2719	1.3548	2.6545	3.9531	5.2360
	Tap	1	0.02812	0.08318	0.17314	0.22018	0.16386	0.41412	0.57984	0.78724
		4	.11360	.24531	.41309	.54508	.08040	.25054	.33610	.46483
		2	.05388	.13209	.24546	.31816	.13873	.36486	.50632	.69004
Pressure, psi		3	.09702	.21393	.36660	.48214	.09652	.28222	.38334	.52730
		1	.02813	.08320	.17317	.22020	.16385	.41410	.57980	.78724
		4	.11362	.24529	.41310	.54514	.08042	.25054	.33610	.46483
		2	.05386	.13206	.24546	.31818	.13871	.36480	.50634	.69006
		3	.09710	.21390	.36660	.48212	.09646	.28221	.38335	.52730
		1	.02813	.08318	.17315	.22020	.16385	.41406	.57980	.78722
		4	.11362	.24531	.41308	.54508	.08040	.25052	.33610	.46483
		2	.05388	.13210	.24546	.31816	.13873	.36480	.50632	.69004
		3	.09708	.21390	.36660	.48214	.09650	.28220	.38336	.52730
Pressure Gradient / Flow rate	Value $\times 10^6$		94234	94222	94238	94225	94222	94221	94236	94141
	Std er $\times 10^6$		19	13	5	10	36	11	9	.....
Kinematic viscosity	Stokes		0.19545	0.19542	0.19545	0.19543	0.19542	0.19542	0.19545	.....

TABLE A2. *Flow rate and pressure data for day 2.*

Flow direction			Right to left				Left to right			
Run number			9	12	13	16	10	11	14	15
	Nominal		1.5	3	4.5	6	1.5	3	4.5	6
Flow Rate, g/s	Mass (g)		164.799	248.408	427.531	521.915	159.538	316.214	415.209	505.133
	Time (s)		107.24	94.47	94.92	98.72	118.38	108.20	105.28	96.45
	Mass (g)		146.345	278.677	470.861	565.833	134.698	275.726	375.640	556.020
	Time (s)		95.23	105.98	104.55	107.02	99.92	94.34	95.24	106.17
	Average		1.5386	2.6326	4.5093	5.2933	1.3495	2.9261	3.9487	5.2434
Pressure, psi	Tap	1	0.02750	0.08296	0.17316	0.21586	0.16358	0.41372	0.57895	0.78789
		4	.12234	0.24524	0.45112	0.54216	0.08046	0.23340	0.33552	0.46466
		2	.05609	0.13194	0.25696	0.31424	0.13858	0.35937	0.50552	0.69050
		3	.10394	0.21377	0.39722	0.47888	0.09656	0.26837	0.38269	0.52730
		1	0.02750	0.08298	0.17318	0.21586	0.16360	0.41376	0.57893	0.78789
		4	.12234	0.24524	0.45114	0.54214	0.08048	0.23344	0.33553	0.46468
		2	.05609	0.13194	0.25700	0.31426	0.13860	0.35946	0.50556	0.69049
		3	.10392	0.21377	0.39724	0.47888	0.09658	0.26840	0.38269	0.52730
		1	0.02750	0.08298	0.17318	0.21586	0.16362	0.41382	0.57892	0.78789
		4	.12232	0.24520	0.45114	0.54216	0.08048	0.23346	0.33552	0.46466
		2	.05606	0.13192	0.25700	0.31426	0.13862	0.35946	0.50552	0.69050
		3	.10394	0.21376	0.39724	0.47888	0.09660	0.26842	0.38270	0.52732
Pressure Gradient / Flow Rate	Value×10^6		94217	94213	94237	94238	94207	94229	94244	94252
	Std er×10^6		10	22	14	16	9	10	3	10
Kinematic viscosity	Stokes		0.19541	0.19540	0.19545	0.19545	0.19539	0.19543	0.19547	0.19548

TABLE A3. *Positions of pressure taps*

Tap No.	Distance (meters)
1	0.93434
2	.73731
3	.40711
4	.28030

7. References

[1] Swindells, J. F., Coe, J. R., and Godfrey, T. B., Absolute viscosity of water at 20 °C, J. Res. NBS **48**, No. 1, 1–31 (1952) RP2279.

[2] Kearsley, E. A., An analysis of an absolute torsional pendulum viscometer, Trans. Soc. Rheol. **3**, 69–80 (1959).

[3] White, H. S., Kearsley, E. A., An absolute determination of viscosity using a torsional pendulum, J. Res. Nat. Bur. Stand. (U.S.), **75A** (Phys. and Chem.), No. 6, 541–551 (Nov.-Dec. 1971).

[4] Tate, D. R., Acceleration Due to Gravity at the National Bureau of Standards, Nat. Bur. Stand. (U.S.), Monogr. 107, 24 pages (June 1968).

[5] Hardy, R. C., NBS Viscometer Calibrating Liquids and Capillary Tube Viscometers, Nat. Bur. Stand. (U.S.), Monogr. 55, 22 pages (Dec. 1962).

[6] Marvin, R. S., The accuracy of viscosity measurements of liquids, J. Res. Nat. Bur. Stand. (U.S.), **75A**, (Phys. and Chem.), No. 6, 535–540 (Nov.-Dec. 1971).

[7] Handbook of Mathematical Functions, Nat. Bur. Stand. (U.S.), Appl. Math. Ser. 55, p. 258 (June 1964).

(Paper 75A6–686)